Journal of Alloys and Compounds 476 (2009) 908–912

Contents lists available at ScienceDirect

Journal of Alloys and Compounds

journal homepage: www.elsevier.com/locate/jallcom

ZnO nanotriangles: Synthesis, characterization and optical properties

Masoud Salavati-Niasari[a,b,*], Noshin Mir[b], Fatemeh Davar[b]

[a] Institute of Nano Science and Nano Technology, University of Kashan, Kashan, P.O.Box 87317-51167, Islamic Republic of Iran
[b] Department of Chemistry, Faculty of Science, University of Kashan, Kashan, P.O.Box 87317-51167, Islamic Republic of Iran

ARTICLE INFO

Article history:
Received 5 May 2008
Received in revised form
20 September 2008
Accepted 27 September 2008
Available online 20 November 2008

Keywords:
Nanostructured materials
Inorganic materials
Chemical synthesis

ABSTRACT

Zinc oxalate, $[Zn(C_2O_4)\cdot 2H_2O]$ was used as a precursor to prepare zinc oxide nanotriangles by thermal decomposition. The different combinations of triphenylphosphine, and oleylamine were added as surfactants to control the particle size. The products were characterized by X-ray diffraction (XRD), transmission electron microscopy (TEM), photoluminescence spectroscopy (PL), Fourier transform infrared (FT-IR) spectroscopy, Ultraviolet–visible (UV–vis) spectroscopy and X-ray photoelectron spectroscopy (XPS). The synthesized ZnO nanoparticles have a hexagonal zincite structure.

1. Introduction

In recent years, there has been an increasing interest in developing materials with low-dimensional nanostructure such as nanotubes and nanocrystals due to their potential technological applications in nanoscale devices [1–4]. It has been obvious that their properties depend sensitively on their size and shape. Therefore, the challenges in nanocrystals synthesis are to control not only the crystal size but also the shape and morphology [5,6].

Zinc oxide is a material of particular interest because of its unique optical and electronic properties. ZnO is a wide bandgap semiconductor (3.37 eV) and has a large excition binding energy of 60 meV, which is also luminescent, and has emerged as a good candidate for many applications. Nanosized ZnO has great potentiality for being used in preparing solar cell [7,8], gas sensors [9], chemical absorbent [10] varistors [11], electrical and optical devices [12], electrostatic dissipative coating [13], catalysts for liquid phase hydrogenation [14], and catalysts for photo-catalytic degradation [15] instead of titania nanoparticles [16].

In the past decade, various different physical or chemical synthetic approaches have been developed to produce ZnO, including vapor phase oxidation [17], thermal vapor transport and condensation (TVTC) [18,19], chemical vapor deposition (CVD) [20], precipitation [21–23], sol–gel [24,25], microemulsion [26], hydrothermal [27], solvothermal [28] and sonochemical methods [29].

Among various techniques for synthesis of ZnO nanoparticles, thermal decomposition is one of the most common to produce stable monodisperse suspensions with the ability of self-assembly. Nucleation occurs when the metal precursor is added into a heated solution in the presence of surfactant, while the growth state take place at a higher reaction temperature [30]. ZnO nanostructures can also be synthesized from different precursors [31,32]. Choi et al. [33] reported a method for the large-scale synthesis of uniform-sized hexagonal pyramid-shaped ZnO nanocrystals by the thermolysis of Zn–oleate complex. Zinc acetylaceton has been reported to be a good precursor for ZnO nanoparticles from thermal decomposition. Salavati-Niasari et al. [34] have synthesized uniform ZnO nanoparticles with size 12 nm by thermal decomposition of zinc acetylacetonate in oleylamine. And so, monodisperse ZnO nanoparticles were successfully prepared through the decomposition of zinc acetylacetonate precursor [35]. Recently Ahmad et al. [36] have synthesized zinc oxide nanoparticles with average size 55 nm by thermal decomposition of zinc oxalate, which were prepared with emulsion method involving cetyltrimethyl ammonium bromide (CTAB) as the surfactant. Kanade et al. [37] have investigated the effect of particle size of ZnO synthesized via thermal decomposition of zinc oxalate at 450 °C. Muruganandham and Wu [38] have reported synthesis of ZnO nanobundles from zinc oxalate by decomposition at 400 °C for 12 h. We decided to prepare ZnO nanocrystals from zinc oxalate at the less temperature and shorter time than the last works done by others. However, an improvement in the thermal decomposition process should be made in preparing ZnO nanotriangles with uniform size in order to extend the appli-

---

* Corresponding author at: Institute of Nano Science and Nano Technology, University of Kashan, Kashan, P.O. Box 87317-51167, Islamic Republic of Iran.
Tel.: +98 361 5555333; fax: +98 361 5552935.
E-mail address: salavati@kashanu.ac.ir (M. Salavati-Niasari).

0925-8388/$ – see front matter © 2008 Elsevier B.V. All rights reserved.
doi:10.1016/j.jallcom.2008.09.196

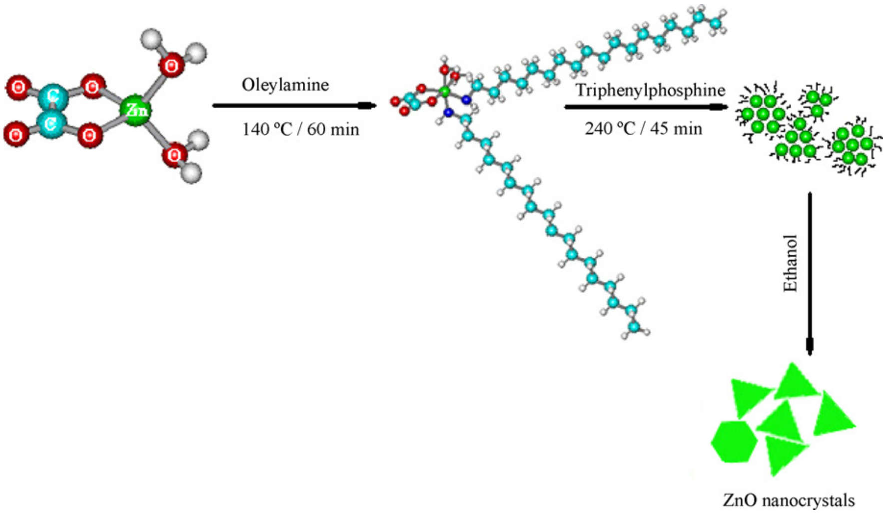

Scheme 1. Schematic depiction of the selective formation ZnO nanocrystals with triangle shapes and hexagonal in shapes by thermal decomposition.

cation areas and satisfy the needs of fundamental research. To the best of our knowledge the used of zinc oxalate as precursor in thermal decomposition at 240 °C is the first time. Here, we report a simple, green, low-cost, and reproducible process for the synthesis of ZnO nanotriangles from zinc oxalate, $[Zn(C_2O_4)\cdot 2H_2O]$, as precursor. In this process, oleylamine was used as both the medium and the stabilizing reagent.

2. Experiment

2.1. Materials

All the chemicals reagents used in our experiments were of analytical grade and were used as received without further purification. Zinc oxalate, $[Zn(C_2O_4)\cdot 2H_2O]$, precursor was synthesized according to this procedure: the 10 mmol of zinc acetate dihydrate $Zn(CH_3COO)_2\cdot 2H_2O$ was dissolved into 10 mL of distilled water to form a homogeneous solution. A stoichiometric amount of potassium oxalate dissolved in an equal volume of distilled water was dropwise added into the above solution under magnetic stirring. The solution was stirred for about 15 min and an orange precipitate was isolated, washed and dried at 50 °C. The obtained product was characterized by FT-IR and elemental analyses.

2.2. Characterization

X-ray diffraction (XRD) patterns were recorded by a Rigaku D-max C III, X-ray diffractometer using Ni-filtered Cu Kα radiation. Elemental analyses were obtained from Carlo ERBA Model EA 1108 analyzer. Transmission electron microscopy (TEM) image and energy dispersive X-ray (EDX) was obtained on a Philips EM208 transmission electron microscope with an accelerating voltage of 200 kV. Fourier transform infrared (FT-IR) spectra were recorded on Shimadzu Varian 4300 spectrophotometer in KBr pellets. The electronic spectra of the complexes were taken on a Shimadzu Ultraviolet–visible (UV–vis) scanning spectrometer (Model 2101 PC). Room temperature photoluminescence (PL) was studied on an F-4500 fluorescence spectrophotometer. X-ray photoelectron spectroscopies (XPS) of the as-prepared products were measured on an ESCA-3000 electron spectrometer with nonmonochromatized Mg Kα X-ray as the excitation source.

2.3. Experimental

The current synthetic procedure is a modified version of the method developed by Hyeon and others for the synthesis of nanocrystals for metals that employs the thermal decomposition of transition metal complexes [39,40]. The synthetic pathway is shown in Scheme 1. In this synthesis ZnO nanotriangles were prepared by the thermal decomposition of zinc oxalate, $[Zn(C_2O_4)\cdot 2H_2O]$–oleylamine complex as precursor. First, the $[Zn(C_2O_4)\cdot 2H_2O]$–oleylamine complex was prepared by reaction 0.6 g of $[Zn(C_2O_4)\cdot 2H_2O]$ and 5 mL of oleylamine. The mixed solution was placed in a 50 mL three-neck distillation flask and heated up to 140 °C for 60 min. The resulting metal-complex solution was injected into 5 g of triphenylphosphine (TPP) at 240 °C. The color of the solution changed from orange to black, indicating that colloidal products were generated. The black solution was aged at 240 °C for 45 min, and was then cooled to room temperature. The white nanocrystals products were precipitated by adding excess ethanol to the solution. The ZnO nanocrystals were washed with ethanol. These products could easily be re-dispersed in nonpolar organic solvents, such as hexane or toluene (Scheme 1). The synthesized nanocrystals were characterized by XRD, TEM, FT-IR, UV–vis and PL techniques.

3. Results and discussion

X-ray powder diffraction pattern of ZnO nanotriangles at room temperature is shown in Fig. 1a. The XRD pattern is consistent with the spectrum of ZnO, and no peak attributable to possible impurities is observed. All of the reflection peaks of the XRD pattern can be indexed well to hexagonal phase ZnO (space group: $P6_3mc$; JCPDS No. 79–0205, with calculated cell parameters $a = 3.24$ Å and $c = 5.18$ Å). The sharp diffraction peaks manifested show that the obtained ZnO nanocrystals have high crystallinity.

The crystallite sizes of the as-synthesized ZnO, D_c, was calculated from the major diffraction peaks of the base of (1 0 1) using the Scherrer formula (Eq. (1)),

$$D_c = \frac{K\lambda}{\beta\cos\theta} \tag{1}$$

where K is a constant (ca. 0.9), λ is the X-ray wavelength used in XRD (1.5418 Å), θ the Bragg angle; β is the pure diffraction broadening of a peak at half-height, that is, broadening due to the crystallite dimensions. The size of the crystallite was estimated from Debye–Scherrer equation [41] is about 30 nm. Chemical purity and stoichiometry of the samples were tested by EDX. The strong peaks related to Zn and O is found in the spectrum Fig. 1b.

Fig. 2 shows a comparison of FT-IR spectrum of (a) $[Zn(C_2O_4)\cdot 2H_2O]$, and (b) ZnO nanotriangles. The broad absorption bands at $\sim$3400 cm^{-1} encompass the O—H stretching vibrations of adsorbed water [42] on the ZnO surface. The spectrum also contains one strong absorption bands at 425 cm^{-1} which confirms the stretching vibration ZnO (ν ZnO) bands [43]. The spectrum of ZnO nanotriangles, (curve b), shows two weak stretch vibrations at 2921 cm^{-1} and 2865 cm^{-1} attributing to the C—H stretching models of the oleylamine carbon chain[35], indicating oleylamine molecules are absorbed on the surface of ZnO nanocrystals. There was no evidence of free precursor, $[Zn(C_2O_4)\cdot 2H_2O]$ in the sample, because stretch vibration of C═O ($\upsilon_{C=O}$) and C—O (υ_{C-O}) oxalate disappeared [44]. So the oleylamine serves as the capping ligand that controls growth [40].

Fig. 3 shows the TEM images of the ZnO nanocrystals. The TEM image (Fig. 3) shows ZnO nanotriangles with an average size of 31 nm.

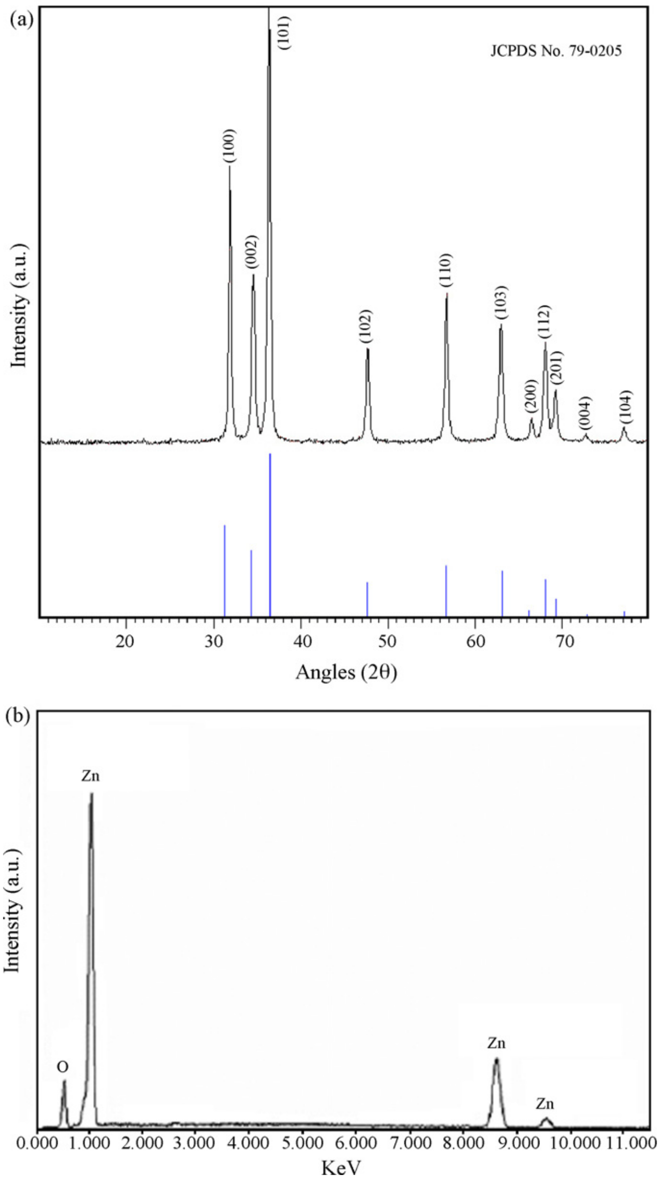

Fig. 1. (a) XRD pattern of the ZnO nanotriangles (the bottom bars shows the standard ZnO from JCPDS No. 79–0205) and (b) EDX spectrum of the ZnO nanotriangles.

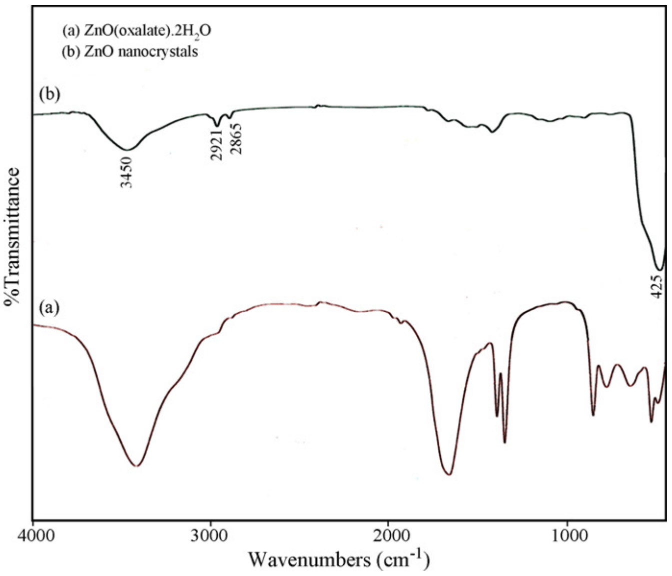

Fig. 2. FT-IR spectra of (a) Zn(oxalate)·$2H_2O$ and (b) ZnO nanotriangles.

The growth mechanism could be well understood on the basis of the following reactions and the crystal habits of triangular ZnO. In the presence of oleylamine as solvent, [Zn(C_2O_4)]–oleylamine were synthesized. After addition of triphenylphosphine (TPP) to these solutions at high temperature, [Zn(C_2O_4)]–oleylamine were decomposed. TPP was widely used in the synthesis of phosphine-stabilized gold or other metal nanoparticles. The phenyl groups in TPP can provide greater steric hindrance than straight-chained alkyl groups such as tributyl and trioctyl to control the size of metal nanoparticles [45]. The addition of TPP into the mixture of oleylamine and complex as an additional surfactant reduced the particle size much further and resulted in nanocrystals with very thin arrays. Oleylamine is known as a ligand that binds tightly to the metal nanoparticles surface. The combined effects of TPP and oleylamine were much more profound than those of individual contributions. When the triphenylphosphine (TPP) was used as the complexing agent, the circumference of produced nuclei was capped by this surfactant, leading to the increase of surface energy of some crystallographic faces. The growth of the ZnO nanocrystals with triangle shapes and hexagonal in shapes can be explained on the basis of the schematic view presented in Scheme 1 [46].

Optical properties of the ZnO nanotriangles were investigated by UV–vis spectra and photoluminescence (PL) spectroscopy at room temperature (Fig. 4). Fig. 4a illustrates the UV–vis absorption spectrum of the nanotriangles which has a red-shift (379 nm) compared to that of bulk ZnO (∼370 nm). This red-shift can be explained by the formation of shallow levels inside the bandgap due to impurity atoms present in the lattice [47]. The PL spectra Fig. 4b shows a near band-edge emission observed at about 383 nm and a relatively broad blue-green emission band at about 472 nm. The UV emission at 379 nm was similar to the bulk bandgap at 383 nm of the ZnO, which originated from the recombination of free excitons [33,48]. A broad blue-green emission band above 472 can be related to a singly charged oxygen vacancy, which results from the recombination of a photo generated hole with a charge state of the specific defect, such as oxygen vacancies, or resulted from the surface deep-level [49,50].

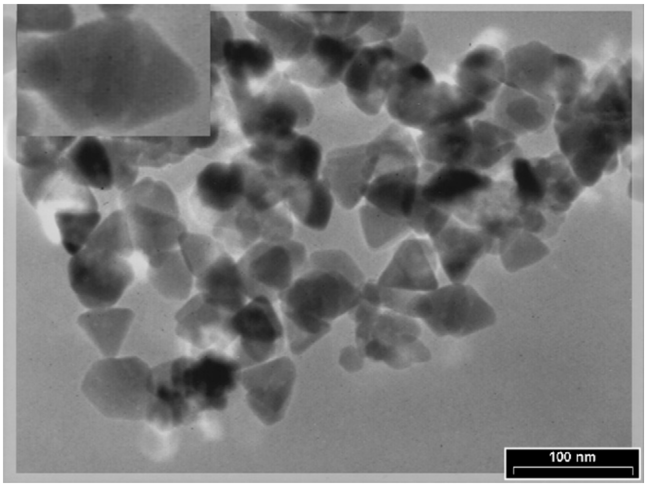

Fig. 3. TEM image of ZnO nanotriangles.

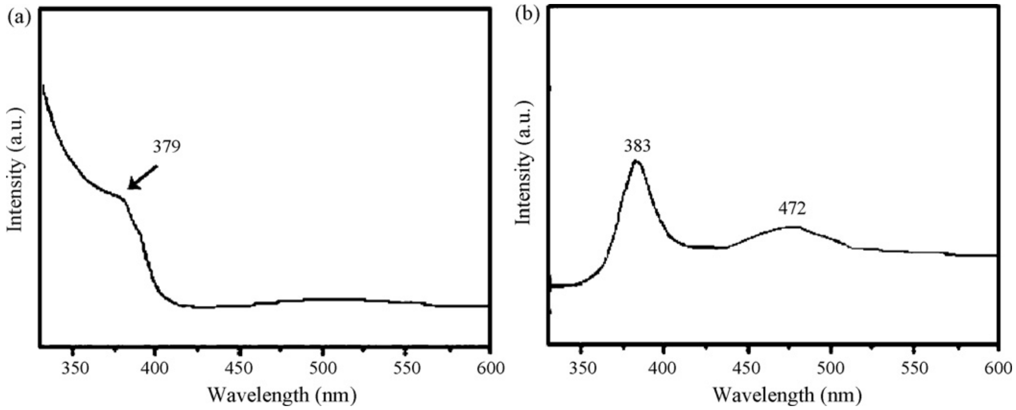

Fig. 4. (a) UV–vis absorption and (b) room temperature PL spectra of the ZnO nanotriangles.

It is known that the large specific surface nanoparticles are important in catalysis. Therefore, the products were characterized by X-ray photoelectron spectroscopy (XPS) to analyze the surface of the products. Fig. 5 shows the XPS for the as-synthesized samples. The XPS gives the binding energies of O 1s, Zn 2p1/2 and Zn 2p3/2 for the as-synthesized ZnO to be 530.5, 1044.5 and 1044.6 eV respectively. A full survey scan did not reveal other element peaks. These results indicate that ZnO nanotriangles have formed. Compared to those for other methods for synthesizing ZnO powders, the conditions for the reaction are very moderate.

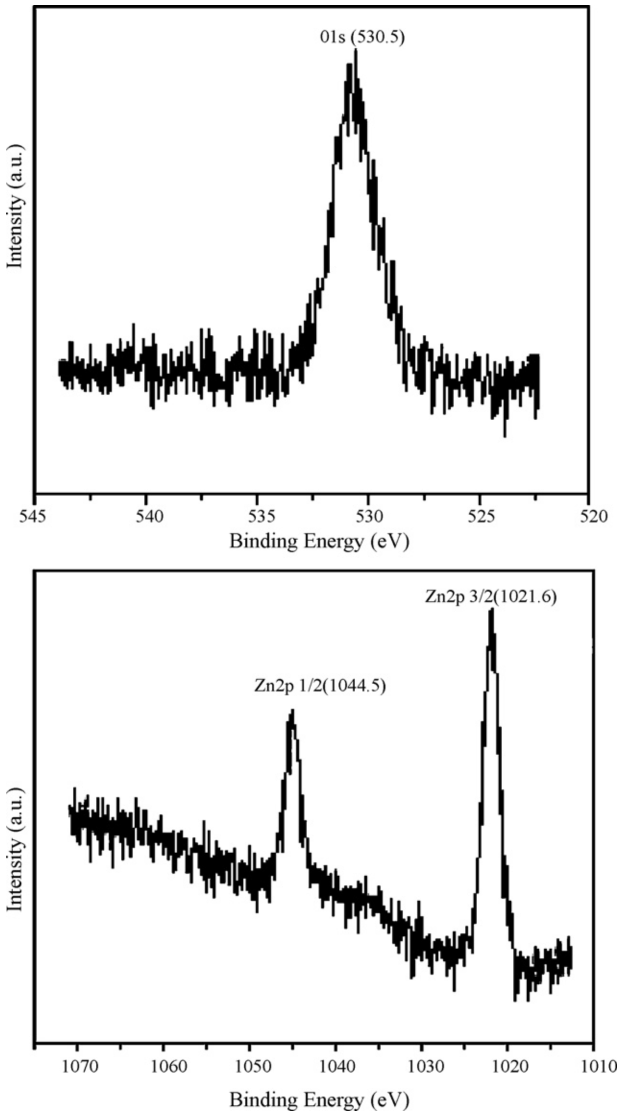

Fig. 5. X-ray photoelectron spectroscopy (XPS) of the as-synthesized ZnO nanotriangles.

4. Conclusion

In summary, ZnO nanotriangles were synthesized via thermal decomposition of [Zn(C_2O_4)]–oleylamine complex. This method employed an inexpensive, reproducible process for the large-scale synthesis of ZnO nanocrystals.

Acknowledgement

Authors are grateful to council of University of Kashan for providing financial support to undertake this work.

References

[1] S. Iijima, Nature 354 (1991) 56.
[2] X. Duan, Y. Huang, R. Agarwal, C.M. Lieber, Nature 421 (2003) 241.
[3] Z.W. Pan, Z.R. Dai, Z.L. Wang, Science 291 (2001) 1947.
[4] H. Huang, S. Mao, H. Feick, H. Yan, Y. Wu, H. Kind, E. Webber, R. Russo, P. Yang, Science 292 (2001) 1897.
[5] J.J. Shiang, A.V. Kadavanich, R.K. Grubbs, A.P. Alivisatos, J. Phys. Chem. 99 (1995) 17417.
[6] S. Ahmadi, Z.L. Wang, T.C. Green, A. Henglein, M.A. Elsayed, Science 272 (1996) 1924.
[7] Z.S. Wang, C.H. Huang, Y.Y. Huang, Y.J. Hou, P.H. Xie, B.W. Zhang, H.M. Cheng, Chem. Mater. 13 (2001) 678.
[8] K. Westermark, H. Rensmo, T.A.C. Lees, J.G. Vos, H.T. Siegbahn, J. Phys. Chem. B 106 (2002) 10108.
[9] H.M. Lin, S.J. Tzeng, P.J. Hsiau, W.L. Tsai, Nanostruct. Mater. 10 (1998) 465.
[10] I. Rosso, C. Galletti, M. Bizzi, G. Saracco, V. Specchia, Ind. Eng. Chem. Res. 42 (2003) 1688.
[11] M. Singhal, V. Chhabra, P. Kang, D.O. Shah, Mater. Res. Bull. 32 (1997) 239.
[12] C. Feldmann, Adv. Fundam. Mater. 13 (2003) 101.
[13] M. Kitano, M. Shiojiri, Powder Technol. 93 (1997) 267.
[14] G.M. Hamminga, G. Mul, J.A. Moulijn, Chem. Eng. Sci. 59 (22–23) (2004) 5479.
[15] M.L. Curridal, R. Comparelli, P.D. Cozzli, G. Mascolo, A. Agostiano, Mater. Sci. Eng. C23 (2003) 285.
[16] G.P. Fotou, S.E. Pratsinis, Chem. Eng. Commun. 151 (1996) 251.
[17] J.Q. Hu, Q. Li, N.B. Wong, C.S. Lee, S.T. Lee, Chem. Mater. 14 (2002) 1216.
[18] J.Y. Lao, J.Y. Huang, D.Z. Wang, Z.F. Ren, Nano Lett. 3 (2003) 235.
[19] J.Y. Lao, J.G. Wen, Z.F. Ren, Nano Lett. 2 (2002) 1287.
[20] J.-J. Wu, S.-C. Liu, J. Phys. Chem. B 106 (2002) 6546.
[21] N.S. Pesika, Z. Hu, K.J. Stebe, P.C. Searson, J. Phys. Chem. B 106 (2002) 6985.
[22] P.V. Radovanovic, N.S. Norberg, K.E. McNally, D.R. Gamelin, J. Am. Chem. Soc. 124 (2002) 15192.
[23] E.W. Seelig, B. Tang, A. Yamilov, H. Cao, R.P.H. Chang, Mater. Chem. Phys. 20 (2003) 257.
[24] P. Hoyer, H. Weller, J. Phys. Chem. 99 (1995) 14096.
[25] G.K. Paul, S. Bandyopadhyay, S.K. Sen, S. Sen, Mater. Chem. Phys. 79 (2003) 71.

[26] L. Gao, Y.L. Ji, H. Xu, P. Simon, Z. Wu, J. Am. Chem. Soc. 124 (2002) 14864.
[27] B. Cheng, E.T. Samulski, Chem. Commun. (2004) 986.
[28] Z. Jia, L. Yue, Y. Zheng, Z. Xu, Mater. Chem. Phys. 107 (2008) 137.
[29] D. Qian, J.Z. Jiang, P.L. Hansen, Chem. Commun. (2003) 1078.
[30] K. Simeonidis, S. Mourdikoudis, M. Moulla, I. Tsiaoussis, C.M. Boubeta, M. Angelakeris, C.D. Samara, O. Kalogirou, J. Magn. Magn. Mater. 316 (2007) e1.
[31] Y.C. Zhang, X. Wu, X.Y. Hu, R. Gao, J. Cryst. Growth 280 (2005) 250.
[32] X.J.X. Duan, X.T. Huang, E.K. Wang, H.H. Ai, Nanotechnology 17 (2006) 1786.
[33] S.-H. Choi, E.-G. Kim, J. Park, K. An, N. Lee, S.C. Kim, T. Hyeon, J. Phys. Chem. B 109 (2005) 14792.
[34] M. Salavati-Niasari, F. Davar, M. Mazaheri, Mater. Lett. 62 (2008) 1890.
[35] J.F. Liu, Y.Y. Bei, H.P. Wu, D. Shen, J.Z. Gong, X.G. Li, Y.W. Wang, N.P. Jiang, J.Z. Jiang, Mater. Lett. 61 (2007) 2837.
[36] T. Ahmad, S. Vaidya, N. Sarkar, S. Ghosh, A.K. Ganguli, Nanotechnology 17 (2006) 1236.
[37] K.G. Kanade, B.B. Kale, R.C. Aiyer, B.K. Das, Mater. Res. Bull. 41 (2006) 590.
[38] M. Muruganandham, J.J. Wu, Appl. Catal. B: Environ. 80 (2008) 32–41.
[39] H.M. Park, E. Kang, S.U. Son, H.M. Park, M.K. Lee, J. Kim, K.W. Kim, H. Noh, J. Park, C.J. Bae, J. Park, T. Hyeon, Adv. Mater. 17 (2005) 429.
[40] M. Salavati-Niasari, F. Davar, M. Mazaheri, M. Shaterian, J. Magn. Magn. Mater. 320 (2008) 575.
[41] H.P. Klug, L.E. Alexander, X-ray Diffraction Procedures for Polycrystalline and Amorphous Materials, 2nd ed., Wiley, New York, 1974.
[42] K. Nakamoto, Infrared Spectra of Inorganic and Coordination Compound, 4th ed., Chemical Industry Press, Beijing, 1991.
[43] H.M. Ismail, J. Anal. Appl. Pyrol. 21 (1991) 315.
[44] K.G. Kanade, B.B. Kale, R.C. Aiyer, B.K. Das, Mater. Res. Bull. 41 (2006) 590–600.
[45] H.T. Yang, Y.K. Su, C.M. Shen, T.Z. Yang, H.J. Gao, Surf. Interface Anal. 36 (2004) 155–160.
[46] T. Ghoshal, S. Kar, S. Chaudhuri, J. Cryst. Growth 293 (2006) 438.
[47] V. Ischenko, S. Polarz, D. Grote, V. Stavarache, K. Fink, M. Driess, Adv. Funct. Mater. 15 (2005) 1945–1954.
[48] E.M. Wong, P.C. Searson, Appl. Phys. Lett. 74 (1999) 2939.
[49] K. Vanheusden, W.L. Warren, C.H. Seager, D.R. Tallant, J.A. Voigt, B.E. Gande, J. Appl. Phys. 79 (1996) 7983.
[50] Y. Li, G.S. Cheng, L.D. Zhang, J. Mater. Res. 15 (2000) 2305.